JOURNAL OF AEROSOL MEDICINE AND PULMONARY DRUG DELIVERY
Volume 26, Number 5, 2013

Pp. 266–279
DOI: 10.1089/jamp.2012.1006

High-Efficiency Generation and Delivery of Aerosols Through Nasal Cannula During Noninvasive Ventilation

P. Worth Longest, PhD,[1,2] Ross L. Walenga, BS,[1] Yoen-Ju Son, PhD,[2] and Michael Hindle, PhD[2]

Abstract

Background: Previous studies have demonstrated the delivery of pharmaceutical aerosols through nasal cannula and the feasibility of enhanced condensational growth (ECG) with a nasal interface. The objectives of this study were to develop a device for generating submicrometer aerosols with minimal depositional loss in the formation process and to improve aerosol delivery efficiencies through nasal cannulas.
Methods: A combination of *in vitro* experiments and computational fluid dynamics (CFD) simulations that used the strengths of each method was applied. Aerosols were formed using a conventional mesh nebulizer, mixed with ventilation gas, and heated to produce submicrometer sizes. An improved version of the mixer and heater unit was developed based on CFD simulations, and performance was verified with experiments. Aerosol delivery was considered through a commercial large-bore adult cannula, a divided (D) design for use with ECG, and a divided and streamlined (DS) design.
Results: The improved mixer design reduced the total deposition fraction (DF) of drug within the mixer by a factor of 3 compared with an initial version, had a total DF of approximately 10%, and produced submicrometer aerosols at flow rates of 10 and 15 L/min. Compared with the commercial and D designs for submicrometer aerosols, the DS cannula reduced depositional losses by a factor of 2–3 and retained only approximately 5% or less of the nebulized dose at all flow rates considered. For conventional-sized aerosols (3.9 and 4.7 μm), the DS device provided delivery efficiencies of approximately 80% and above at flow rates of 2–15 L/min.
Conclusions: Submicrometer aerosols can be formed using a conventional mesh nebulizer and delivered through a nasal cannula with total delivery efficiencies of 80–90%. Streamlining the nasal cannula significantly improved the delivery efficiency of both submicrometer and micrometer aerosols; however, use of submicrometer particles with ECG delivery resulted in overall lower depositional losses.

Key words: Noninvasive ventilation aerosol delivery, nasal high-flow therapy, enhanced condensational growth aerosol delivery, controlled condensational growth, mesh nebulizers, submicrometer aerosols, computational fluid dynamics, *in vitro* aerosol testing

Introduction

Both noninvasive positive pressure ventilation (NPPV) and high-flow therapy (HFT) with nasal interfaces are popular forms of ventilation support to treat respiratory insufficiency.[1–4] Nasal HFT involves the continuous delivery of air or blended oxygen to the nose using a cannula interface.[4,5] The air is heated and humidified to improve comfort and allow for flow rates of 10–60 L/min in adults. Compared with mask delivery or usual care, patients receiving nasal HFT had improved blood oxygenation, respiratory rates, and quality of life scores.[2,4,6,7] As with other forms of noninvasive ventilation (NIV), patients receiving nasal NPPV or HFT often have underlying lung or systemic conditions that may be improved with the use of pharmaceutical aerosols.[8–10] Ideally, the aerosol should be administered without interrupting the delivery of the ventilation gas.[8–10] Aerosol delivery to the lungs through a nasal cannula interface has the added advantage of convenience for medications with long delivery times or medications that must be administered frequently or continuously due to short durations of action. However, aerosol delivery efficiencies through nasal interfaces during

[1]Department of Mechanical and Nuclear Engineering, Virginia Commonwealth University, Richmond, VA 23284.
[2]Department of Pharmaceutics, Virginia Commonwealth University, Richmond, VA 23298.

both NPPV and HFT are expected to be low due to high flow rates, humidification, small delivery line diameters, and nasal cannulas with narrow flow passages and abrupt changes in flow direction.

Due to these expected high depositional losses, previous studies on nasal cannula aerosol delivery have focused on pediatric patients and low flow rates. Bhashyam *et al*.[11] considered aerosol delivery from a mesh nebulizer (Aeroneb Solo, Aerogen Limited, Galway, Ireland) through infant, pediatric, and adult nasal cannulas at an inspiratory flow rate of 3 L/min with a heated and humidified system. Depositional losses in the connectors, tubing, and cannula resulted in a total output that ranged from 18.6% to 26.9% of the initial dose when airflow was included in the system. Ari *et al*.[12] considered aerosol delivery from the Aeroneb Solo device through an Optiflow (Fisher & Paykel, Irvine, CA) pediatric nasal cannula at flow rates of 3 and 6 L/min with oxygen or heliox. The maximum cannula aerosol delivery efficiency of approximately 10% occurred with a flow rate of 3 L/min and was decreased significantly with the use of the higher flow rate and heliox. For both of these studies, delivery rates to the lung are expected to be significantly lower than the fraction exiting the cannula interface due to deposition in the nasal airways.[13–15] Depositional losses in nasal cannulas at higher flow rates consistent with NPPV and HFT for adults and for different particle sizes have previously not been reported. The administration of pharmaceutical aerosols during other forms of NIV was previously reviewed[8–10,16] and indicated typical patient delivery rates of less than 1–10% from *in vitro* studies and 1–6% under *in vivo* conditions.

Longest *et al*.[15] recently proposed the concept of enhanced condensational growth (ECG)[17,18] to improve the lung delivery of nasally administered aerosols during HFT. Aerosol deposition and size increase were evaluated in an adult nose–mouth–throat (NMT) replica geometry using both *in vitro* experiments and computational fluid dynamics (CFD) simulations. For the ECG nasal delivery approach, separate streams of a submicrometer aerosol and warm (39°C) saturated air were generated and delivered to the right and left nostril inlets, respectively. The small aerosol size minimizes depositional losses in the interface device and extrathoracic airways. Condensational growth then occurs when the aerosol and humidity streams combine in the nasopharynx and continue downstream. In the study of Longest *et al*.,[15] both *in vitro* results and CFD predictions indicated that, with ECG delivery, depositional losses in the NMT region were approximately 15% at a total flow rate of 30 L/min through the model, and condensational growth increased the initially submicrometer aerosol size to approximately 2 μm in the trachea. In comparison, deposition of a conventional 4.7-μm aerosol in the NMT geometry was found to be approximately 70% under identical flow conditions. By increasing the aerosol stream inlet temperature in the CFD model, total depositional losses in the NMT were reduced to 5%. Based on this study, ECG was shown to significantly improve the delivery of pharmaceutical aerosols to the lungs during nasal administration with high flow rates and to achieve conventional aerosol size upon entering the lungs. Hindle and Longest[18] and Tian *et al*.[19] demonstrated continuing size increase of aerosols downstream of the trachea during ECG aerosol delivery with oral inhalation. The growth occurred within a timescale that was sufficient to result in predicted full lung retention of the aerosol. Size increase of the aerosol may be further enhanced with the use of hygroscopic growth excipients.[20–22] One limitation of the nasal delivery study by Longest *et al*.[15] was the use of an unrealistic nasal cannula interface that was only intended to route the aerosol to the nostrils in the experiments. Therefore, depositional losses in realistic or practical nasal cannulas were not considered. Furthermore, a small-particle aerosol generator (SPAG) was used in the experiments to generate the unheated aerosol stream with a flow rate of 10 L/min and a delivery temperature of 21°C or less. For delivery during HFT, heating and providing some humidification to the carrier gas are required.

To facilitate the use of submicrometer and nanometer aerosols combined with controlled condensational growth, Longest *et al*.[23] considered the formation of submicrometer particles from conventional mesh nebulizers. A radial mixer design was used to combine a gas delivery stream with aerosols produced from the Aeroneb Pro and Aeroneb Lab nebulizers (Aerogen). Aerosol size was decreased by drying in a 1-m tube with and without wall heating. Through an appropriate selection of flow rates, nebulizers, and model drug concentrations, submicrometer aerosols could be formed with the three drying devices considered. A wire heated design was shown to overheat the airstream, producing unsafe conditions for inhalation if the aerosol was not uniformly distributed in the tube cross section or if the nebulizer stopped producing droplets. In comparison, a counterflow heated design provided sufficient thermal energy to produce submicrometer particles, but also automatically limited the maximum outlet temperature for inhalation based on the physics of heat transfer. Depositional losses in the mixer and tubing were not evaluated, but were expected to be high based on drug recovery during impactor testing.

As described, previous studies have indicated the effectiveness of ECG aerosol delivery through a nasal interface and the feasibility of using conventional mesh nebulizers to form submicrometer aerosols. To allow for efficient aerosol delivery during nasal HFT, a novel device is needed that can generate a submicrometer aerosol and deliver it through a nasal cannula interface with minimal depositional loss. As a performance goal for this novel device, depositional loss of drug should be below 10% of the initial nebulized dose in both the submicrometer aerosol mixer with connective tubing and nasal cannula interface with connective tubing, resulting in a total delivery efficiency of greater than 80% through the system. To maintain continuous ventilation support during HFT in adults, the effective operating range of the device should be approximately 10–15 L/min. The system should also provide heating of the airstream and increase the relative humidity (RH) of the ventilation gas to ensure patient comfort during the delivery period. Finally, the optimal aerodynamic particle size for ECG nasal delivery should be approximately 900 nm, which provides a good balance between low NMT deposition[15] and high drug payload delivery.

The objective of this study was to improve the delivery of medical aerosols during NIV from the site of droplet formation through delivery to the patient with a nasal cannula. As described above, the delivery system of interest consists of a mixer capable of forming a warmed submicrometer

aerosol, connective tubing, and a nasal cannula interface. Flow rates considered range from typical values used with low-flow gas delivery (~2–5 L/min) through conventional values used for HFT (~10–30 L/min). A combination of *in vitro* experiments and CFD simulations is applied that uses the strengths of each method to accelerate the design and development process. Aerosols are formed using a conventional mesh nebulizer, mixed with ventilation gas, and heated to produce submicrometer sizes. Deposition in an initial radial mixer design is first considered to establish the need for reducing aerosol losses and to validate the CFD model predictions. Based on CFD simulations, an improved version of the mixer is then developed that uses counterflow heating of the aerosol stream, a larger aerosol reservoir, and a more compact heating section compared with the radial mixer design. Performance of the improved design is assessed using CFD simulations of both aerosol evaporation and deposition. *In vitro* experiments are used to validate drug deposition predictions of submicrometer and micrometer particles in an adult Optiflow nasal cannula over a range of flow rates. Additional cannula designs are then proposed to facilitate aerosol delivery with ECG and reduce cannula depositional losses. Finally, the improved mixer and nasal cannula are fabricated and tested experimentally to determine drug depositional losses and verify the formation of an aerosol with an optimal 900-nm mass median aerodynamic diameter (MMAD).

Materials and Methods

Devices to form submicrometer aerosols

To form the aerosol, the Aeroneb Lab nebulizer (Aerogen) was selected, which implements a vibrating mesh with micro-orifices. Performance of the Aeroneb Lab device was previously reported by Longest *et al.*[23] and includes a liquid aerosolization rate of 0.2 mL/min, an initial aerosol MMAD of 3.9 μm, and a particle number concentration of 4.28×10^5 part/cm^3 in an airflow of 15 L/min based on a monodisperse aerosol approximation. The mesh nebulizer output is combined with ventilation gas using a mixing apparatus. Thoughtful design of the mixing unit is required to minimize deposition due to turbulence, momentum of the aerosol stream, and inertia of the micrometer droplets. The previous study of Longest *et al.*[23] considered a radial mixer design where inlet ventilation gas was combined with the aerosol using a porous shell characterized by 2-mm holes (Fig. 1a). The unit was relatively compact with an approximate 4-cm inlet diameter and 8-mm outlet inner diameter that connected with 10-mm tubing. Based on CFD predictions, use of an unheated ventilation gas was insufficient to dry the aerosol at flow rates of 15 L/min and below. To form the submicrometer aerosol and condition the airstream for inhalation, a 1-m segment of tubing was used with counterflow heating (not shown). The counterflow airstream was exhausted as waste so that the previous radial system required two gas inputs. At higher flow rates, deposition was expected in the radial mixer due to the small outlet diameter, turbulence from the porous wall, and momentum of the aerosol stream.

To minimize deposition in the mixer unit, CFD was implemented for the development of an improved design. Design enhancements were specified to include a larger reservoir to hold the aerosol, a compact heat exchanger region, and recirculation of the heated air through the system. Preliminary simulations indicated that a radial cross section provided insufficient heat transfer for a compact heat exchanger design. Furthermore, perforated walls introduced unnecessary turbulence into the system, which increased aerosol deposition especially between the perforations. The improved mixing and heating unit was determined to have a rectangular design with a vertical orientation, a channel-based heat transfer region, and recirculating air entering as far as possible from the mesh nebulizer (Fig. 1b). The aerosol first enters the mixing region, is entrained by predominately laminar airflow, and then enters the narrow heat-transfer channel (Fig. 1b). The combined mixing and heating unit is referred to simply as the improved aerosol mixer for the remainder of this study.

Features of the optimal mixer design include introduction of the aerosol through an approximate 2.4-cm diameter

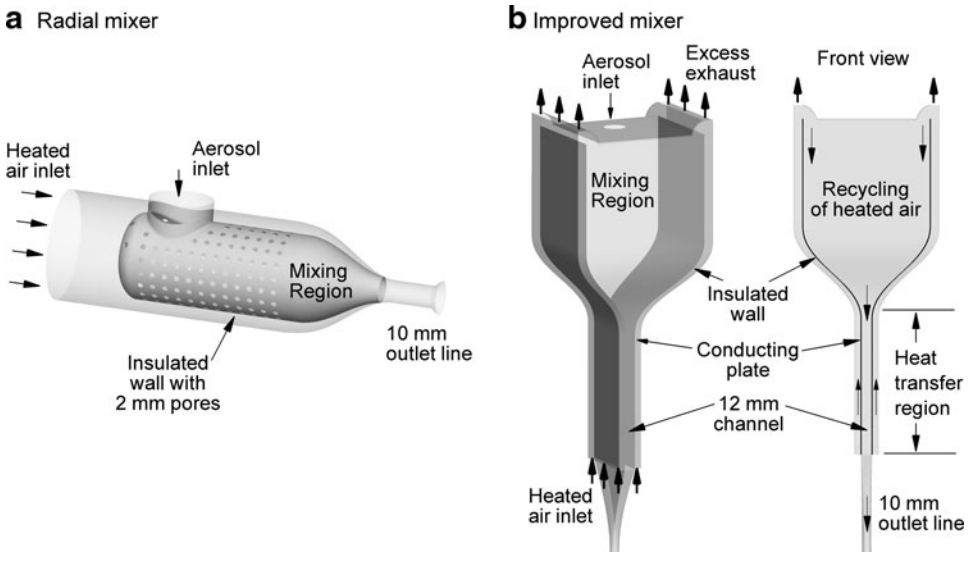

FIG. 1. Aerosol mixers including the **(a)** radial mixer and **(b)** improved mixer designs. The aerosol is supplied by an Aeroneb Lab mesh nebulizer. In the radial mixer, downstream counterflow heating is required to evaporate the aerosol. With the improved design, a single heated gas stream is used to heat the conducting walls in the evaporation region and is then combined with the aerosol to enhance evaporation in the mixing region.

opening in the top of the unit. Heated air enters at the bottom of the counterflow heat exchanger using a manifold and travels up the device in 0.7×8 cm channels (Fig. 1b). In the heat exchanger region, conducting plates are used to transfer heat into the central aerosol stream. At the top of the unit, some of the heated air is exhausted to waste while a portion is recirculated for mixing with the aerosol. The combined ventilation gas and aerosol are funneled into a central channel with a cross-sectional profile of 1.2×8 cm. This streamlined and channel-based design minimizes deposition and maximizes heat exchange. The outlet of the heat exchanger region is smoothly connected to ventilator tubing with an approximate diameter of 10 mm. The geometry includes 50 cm of the ventilator tubing, and the initial section has a 90° bend with a 12.4-cm radius of curvature (not shown in Fig. 1b).

As described by Longest *et al.*,[23] the thermal energy needed to evaporate the aerosol requires relatively high flow rates at temperatures that are safe for inhalation. In the improved design, heated air enters the counterflow heat exchanger at a total flow rate of 80 L/min (40 L/min per channel). A specially designed manifold was used to evenly divide the airstream. The counterflow air was supplied by a house compressed air line and measured to be at less than 5% RH. In one version, an inline resistance heater (OMEGALUX AHP-5052; Omega Engineering Inc., Stamford, CT) and voltage regulator were used to heat the inlet air. As an alternative design, Kapton® (OMEGALUX KHLV-202; Omega Engineering Inc.) heaters were placed directly on the conducting plates on the outside of the aerosol heating region. Vents on top of the mixer region were adjusted to control the outflow resistance and recirculate flow rates of 5, 10, or 15 L/min through the device. Recirculating the airflow simplifies the system by requiring only one air input and also provides additional heat to allow for a smaller heat-exchange region to evaporate the aerosol. Based on the venting of excess gas, increased resistance during exhalation at the cannula will reduce flow through the system and potentially allow droplets to collect in the mixing region for inhalation with the next breath.

Cannula designs

To maximize aerosol transport through the cannulas, inlet lines of 10-mm diameter were considered along with conventional large-bore nostril prongs. The Optiflow nasal cannula, which was also considered in the study of Ari *et al.*,[12] was evaluated first. In the current study, the medium-sized adult Optiflow cannula was evaluated with a 10-mm inlet line and approximate outlet prong size of 5-mm diameter (Fig. 2a). Nasal delivery with ECG requires separate streams of humidified gas and aerosol to enter the left and right nostrils. A divided (D) nasal cannula was designed with separate aerosol and humidity air inlets (Fig. 2b). As described in the Introduction, these gas streams remain separate until the nasopharynx, where they begin to mix, creating supersaturated conditions and fostering aerosol size increase. Dimensions of the inlet prongs were again 5 mm for comparison with the Optiflow cannula. Finally, a streamlined flow path for the aerosol was included in the divided cannula. The divided and streamlined (DS) cannula included nasal prongs containing oval outlets with major and minor diameters of 7.5 and 5 mm, respectively (Fig. 2c). The oval shape is expected to reduce recirculating velocity in the cannula and exit velocities at the nose. For all cannulas, inlet aerosol lines were included with a length of 20 cm, diameter of 10 mm, and radius of curvature of 13.1 cm. Tube diameters in the D and DS models were reduced to 8 mm at the inlet of the cannula to accommodate a quick connect feature for aerosol lines in the prototype designs.

Experimental methods

Experiments were conducted to determine the amount of drug aerosol depositing in the original radial mixer design, drug deposition in the Optiflow cannula for submicrometer and micrometer particles, and the performance of the improved mixer used in conjunction with the DS cannula interface. Considering deposition in the radial mixer with counterflow heat exchanger, the Aeroneb Lab nebulizer was used with an aqueous-based solution containing 0.1% w/v albuterol sulfate (AS). Previous experimental measurements have indicated that AS is mildly hygroscopic with a van't

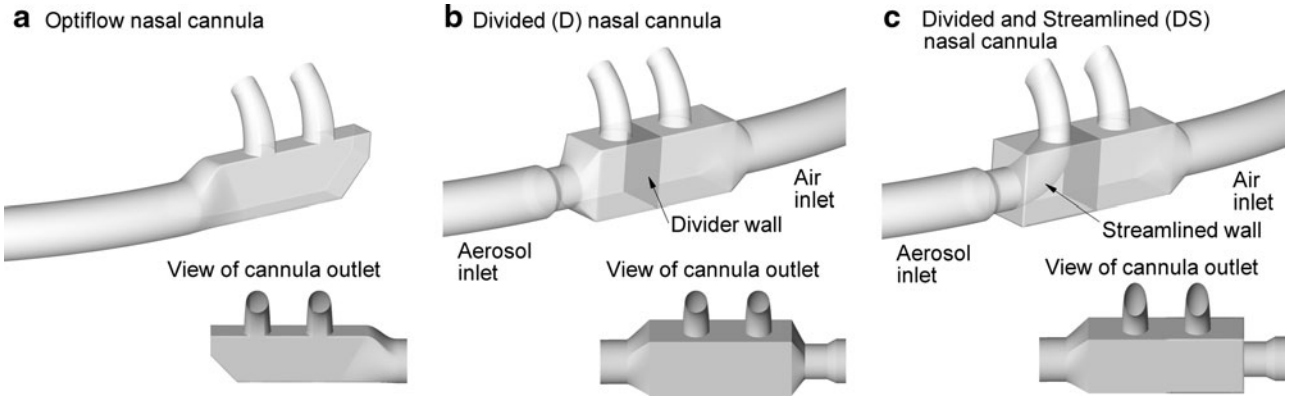

FIG. 2. Cannulas for delivering aerosols during nasal high-flow therapy including the **(a)** Optiflow, **(b)** divided (D) wall, and **(c)** divided and streamlined (DS) designs. Both airflow and the aerosol are delivered through the single inlet of the Optiflow design. The D model allows for delivery of the aerosol and airflow through separate nostrils, which is needed with the ECG approach. The DS design includes a smooth flow pathway for the aerosol stream to decrease depositional loss in the cannula.

Hoff factor of 2.1 and a hygroscopic parameter of 4.9.[21] For comparison, NaCl has a hygroscopic parameter of 77.9, as defined by Longest and Hindle.[21] Aerosol was generated into the radial mixer, which was supplied with 5 or 15 L/min of air at approximately 21°C in separate experiments. A counterflow heat exchanger (not shown in Fig. 1a) was used to dry the aerosol as it exited the radial mixer. Heat exchange took place in a 1-m tube with counterflow air at a flow rate of 80 L/min and temperature of 42°C. Longest *et al.*[23] reported that this setup created a submicrometer aerosol with a MMAD of 0.48 μm [standard deviation (SD) = 0.06] measured using a 10-stage MOUDI (MSP Corp., Shoreview, MN) operated at 30 ± 2 L/min. Makeup air was supplied to the MOUDI from an environmental cabinet (Espec, Hudsonville, MI) to generate the required 30 L/min at a temperature and RH consistent with the stream exiting the radial mixer system. The mesh nebulizer was operated for 50 sec, producing a drug output of 220 μg from the nebulizer. Deposition in the system was established based on the recovered dose in the impactor and the measured nebulized drug output. A validated HPLC-UV method for AS was used to quantify individual stage drug deposition following impaction plate washing using appropriate volumes of water.

Aerosol drug deposition in an adult Optiflow cannula was investigated using two aerosols with differing particle-size characteristics. The Fisoneb nebulizer (Fisons Corp., Rochester, NY) was used to generate a conventionally sized inhalation aerosol with 0.5% AS in water solution. The MMAD of the aerosol was 4.67 (SD = 0.05) μm. Submicrometer aerosols were generated using the SPAG (SPAG-6000; ICN Pharmaceuticals, Costa Mesa, CA). AS solutions were nebulized and dried using the SPAG to produce an aerosol with an initial mean MMAD of 900 (SD = 32.7) nm. This 900-nm aerosol was generated using 0.5% AS in water solution with a nebulizer gas flow rate of 7 L/min and a drying gas flow rate of 3 L/min. Aerosols were generated for 1.0 min into an adult Optiflow cannula with approximately 20 cm of 10-mm diameter tubing. A prototyped streamlined connector was used to join the SPAG outlet to the Optiflow tubing to minimize deposition in this transitional region. The aerosol exiting the nasal cannula was collected on a glass-fiber filter that was connected to a vacuum source operating at 20 L/min. The air supplied to the Fisoneb nebulizer and the additional air supplied to the SPAG to form the 20 L/min flow rate were at ambient conditions. Following aerosol generation, appropriate volumes of water were used to collect AS deposited on the tubing, on the walls of the cannula, and from the filter. The amount of drug deposited was determined by quantitative HPLC AS analysis of the washings. The mean (SD) deposition fraction (DF) results were expressed as a percentage of the total delivered dose of AS.

To verify performance of the improved mixer and DS cannula designs, experiments were conducted to determine both deposition within the system and particle size exiting the mixer. The devices were constructed with CAD software and in-house rapid prototyping facilities. Specifically, a Viper SLA system (3D Systems, Valencia, CA) was used to construct the mixer and cannula using Accura 60 clear plastic resin. The conducting plates in the heat exchanger section were approximately 1-mm thick and constructed out of aluminum. Walls of the mixer and cannula were approximately 2-mm and 1-mm thick, respectively. Based on formulas to predict dried particle size, the initial concentration of AS in the nebulizer solution was estimated to produce an aerosol with a final dried MMAD of approximately 900 nm [mass median diameter (MMD) = 778 nm with ρ_{AS} = 1.34 g/cm^3). Heated air was supplied to the system for approximately 2 min to allow the temperature at the air outlet to reach 39°C. The Aeroneb Lab nebulizer was then turned on and operated for 30 sec to determine deposition in the system, including the nasal cannula. Aerosol exiting the cannula was collected on a glass-fiber filter using an airflow rate of 15 L/min. A second set of experiments was conducted where the aerosol exiting the mixer and 50 cm of tubing was sized using an Andersen Cascade impactor (ACI; Graseby-Andersen Inc., Smyrna, GA). Both deposition and sizing experiments were conducted at a continuous flow rate of 15 L/min. To provide the 30 L/min required by the ACI, makeup air was supplied from an environmental cabinet (Espec) with a temperature and RH similar to those of the aerosol stream entering the impactor. By matching the temperature and RH of the airstream, additional size change of the aerosol was avoided during size measurement. At 30 L/min, the minimum and maximum cutoff diameters of the ACI are 0.43 and 10 μm, allowing for good resolution of the aerosol.

Drug deposition on the nebulizer, tubing, and cannulas and within the ACI was determined following collection of washings using appropriate volumes of deionized water (5–50 mL). The solutions were then assayed using a validated HPLC-UV method for AS. The mass of AS on each impaction plate was determined and used to calculate the aerodynamic particle size distributions of the drug. The MMAD was defined as the particle size at the 50th percentile on a cumulative percent mass undersize distribution (D50) using linear interpolation. The mass of formulation nebulized was determined by weighing the nebulizer before and after each experiment. The solution AS concentration and the mass of formulation nebulized were used to determine the nominal dose of AS delivered. AS system deposition results were reported as a percentage of the nominal delivered dose. Due to experimental difficulties measuring deposition within the mixer, the difference between the nominal dose and the recovered dose was used to estimate the maximum possible AS deposition within the mixer. At least four replicates of each experiment were performed.

Transport modeling and numerical methods

Transport dynamics in both the mixer and cannula geometries include laminar, transitional, and turbulent flows along with multiple phases. Simulations in the mixer system include multiple species (air and water vapor), multiple phases, aerosol size change, strong two-way coupling between the phases, and interactions with the walls. Particles in the cannula geometries were assumed to have reached a final equilibrium size, and further size change was not considered. Flow rates in the mixer geometry include 5, 10, and 15 L/min to simulate nasal HFT and NPPV conditions to a single nostril, as with ECG. In the cannula geometries, aerosol stream flow rates of 2, 5, 10, and 15 L/min were considered along with 20 L/min for the Optiflow system, to evaluate the delivery of both low-flow and high-flow therapy. These flow rates were for the aerosol delivery side of the D and DS

cannulas and the single inlet of the Optiflow cannula. For the mixer, Reynolds numbers ranged between 40.3 in the large upper region at 5 L/min to 2,002.6 in the outlet tube at 15 L/min. In the nasal cannulas, the Reynolds number range was 267–4,005. Longest and Hindle[24] recently described CFD methods for simulating aerosol condensation and evaporation with multicomponent droplets including two-way coupling. These methods were largely used in the current study. For completeness, the CFD methods are briefly reviewed below, with differences from the study of Longest and Hindle[24] highlighted.

To simulate laminar through turbulent conditions, the low Reynolds number (LRN) κ-ω model was selected based on its effectiveness and successful use in previous studies in simulating both aerosol size change and deposition.[22,24–27] The related governing equations for mass and momentum transport along with turbulence variables are available in Wilcox[28] and Longest and Xi.[29] Coupled heat and mass convective-diffusive equations for turbulent flow were previously reported by Longest and Hindle.[24] These expressions include source terms to account for the exchange of heat and water vapor mass between the phases during droplet evaporation. Particle tracking was performed using a Lagrangian approach including terms for drag, gravity, and Brownian motion.[30] The turbulent dispersion of particles was included in both determining the coupled flow-field solution and aerosol deposition. Anisotropic corrections of near-wall turbulence were used to improve the accuracy of the deposition predictions.[31,32] Droplet evaporation and condensation models along with expressions for droplet properties, including hygroscopic effects for multiple solutes, were previously reported by Longest and Hindle.[24]

The commercial CFD package Fluent 12 (ANSYS, Inc., Canonsburg, PA) was used to solve the governing equations in all cases considered. User-supplied Fortran and C programs were implemented for the calculation of initial flow and droplet profiles, hygroscopic droplet evaporation, near-wall anisotropic turbulence approximations, near-wall particle interpolation,[30] Brownian motion,[30] as well as heat and mass sources and sinks during two-way coupling. CFD best practices were used including the use of second or higher order discretization, hexahedral grids,[33] and double-precision calculations. Grid converged results based on negligible change in the velocity and temperature fields (<1% relative error), as well as negligible differences in the outlet droplet size (<5%) and deposition (<5%), were established for a mesh consisting of approximately 1,200,000 control volumes for the improved mixer geometry and approximately 480,000–530,000 control volumes for the nasal cannula.

All CFD results were computed for steady-state conditions. In the initial RH field with one-way coupling, droplets evaporate to dry particles very near the inlet. However, it is the two-way coupling between the discrete and continuous phases that ultimately limits the final size of the aerosol. As a result, the system was found to be extremely sensitive to two-way coupling effects, and a small under-relaxation factor (URF) on the mass and energy source terms was required. For converged solutions, URFs on the source terms ranged from 0.08 to 0.1 with 120 iterations per discrete phase update. Based on the findings of Longest *et al.*,[23] the number of discrete phase updates for a converged solution was estimated to be $2/\text{URF}_{\text{source terms}}$. Increasing the numerator of this expression from 2 to 3 had negligible impact on the predicted transport variables and outlet particle sizes. Stability of the solution was improved by limiting the maximum size a droplet could attain in the initial iterations. This prevented large particle diameter swings and instability as the solution was started. Convergence was determined based on mass, momentum, and energy residuals below 1×10^{-5} at the end of each continuous phase update. Decreasing this convergence criterion by an order of magnitude and increasing the number of continuous phase iterations by a factor of 2 had a negligible impact on the results.

Previous studies have successfully resolved two-way coupled heat and mass transport using the fully polydisperse distribution of various aerosols from experiments.[15,22,24] In this study, as with Longest *et al.*,[23] the MMAD from the experiments was used to define the mean initial aerosol size. This mean initial aerosol size, together with the measured nebulizer liquid output rate, was used to estimate the aerosol number concentrations. For each model, 3,000 droplets with the mean initial size were simulated to predict the multi-way coupled flow fields and outlet particle diameters. DF predictions in both the mixer and nasal cannula were based on 6,000 droplets. Increasing the initial number of representative droplets by an order of magnitude (but keeping the total liquid mass injection rate constant to account for two-way coupling) had a negligible effect on the results.

Results

Radial mixer

Performance of the radial mixer at flow rates of 5 and 15 L/min is illustrated in Figure 3 based on droplet trajectories and deposition locations from CFD predictions. Droplet trajectories at 5 L/min illustrate swirling flow in the mixer with helical paths exiting the device (Fig. 3a). At 15 L/min, an area of low pressure is created in the rear portion of the mixer due to accelerating streamlines passing around the porous inner shell, which pulls the droplet trajectories away from the exit (Fig. 3b). Turbulent fluctuations are also evident in the trajectories at 15 L/min. Some deposition due to impaction is observed in the 5 L/min case along the lower wall of the mixer with a predicted total DF of 7.7%, which is within one SD of the experimental drug deposition of 2.7% (SD = 7.3%) (Fig. 3c). Turbulence induced by the jets at 15 L/min results in more uniform deposition throughout the mixer with a predicted DF = 31.0% and an experimental drug DF = 29.5% (SD = 10.0%) (Fig. 3d). These results indicate that the small radial mixer is adequate at 5 L/min in terms of low deposition. However, aerosol drug deposition at 15 L/min is greater than the target criterion of less than 10% for high-efficiency delivery. Moreover, the CFD predictions were in good agreement with the experimental results for both flow rates considered, which provides confidence in the model for developing the improved design.

Improved mixer

For the improved mixer, contours of velocity, temperature, and RH along with velocity vectors at an outlet flow rate of 15 L/min are illustrated in Figure 4. Inlet air was provided at a temperature of 45°C and flow rate of 80 L/min.

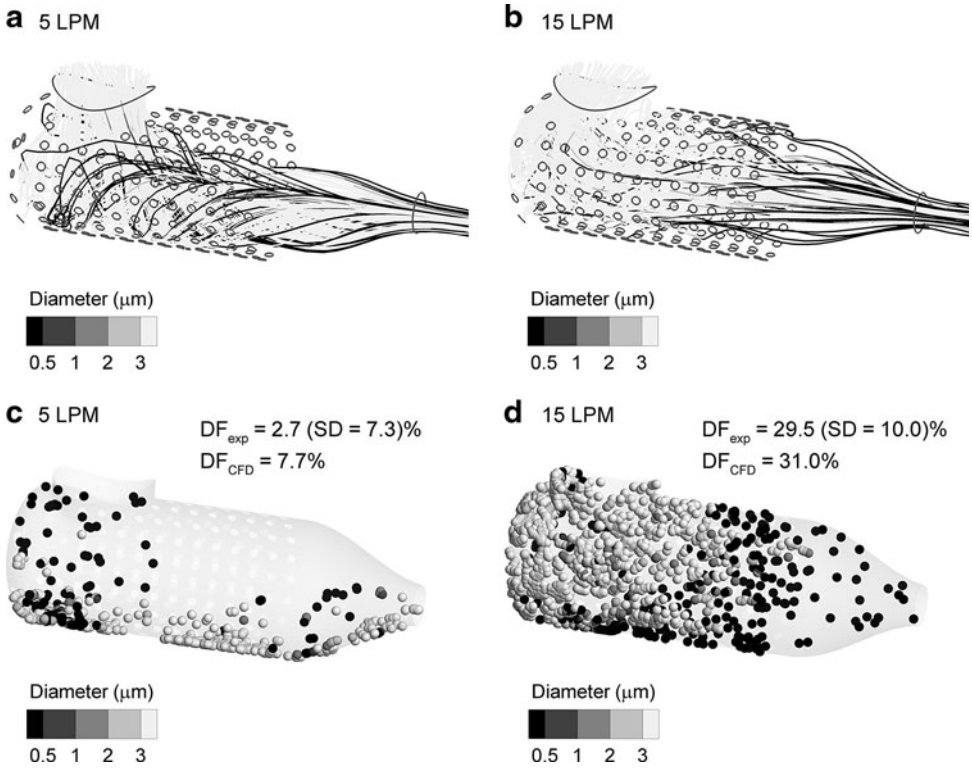

FIG. 3. Performance of the radial mixer in terms of aerosol trajectories shaded according to droplet diameter for flow rates of **(a)** 5 and **(b)** 15 L/min, and aerosol deposition locations shaded according to deposited size for flow rates of **(c)** 5 and **(d)** 15 L/min. DFs predicted by the CFD model are within one SD of the experimental results.

The velocity vectors illustrate recirculation of the heated air into the mixing chamber with minimal high-velocity vortical flow (Fig. 4a). Momentum of the aerosol stream creates a central core of flow through the system. Entrance into the heat exchanger channel causes favorable spreading of the flow and a nearly uniform velocity profile. The core of aerosol flow results in a region of low temperature as evaporation occurs passing through the center of the mixer (Fig. 4b). This core of low temperature expands in the heat exchanger channel region and dissipates. Similarly, RH values are unified and decreased in the heat exchanger region as the aerosol evaporates and the airstream is warmed (Fig. 4c). CFD predicted outlet temperature and RH conditions at the exit of the 50 cm of outlet tubing are 32.0°C and 40.4%, respectively. Table 1 provides outlet temperature and RH values, calculated on a mass-flow-rate–averaged basis, for inlet temperatures of 45°C and 50°C and a range of outlet flow rates.

Trajectories along with deposition locations for the improved mixer are illustrated in Figure 5 at aerosol outflow rates of 5 and 15 L/min and a heated air inlet temperature of 45°C. At 5 L/min, insufficient spreading of the aerosol core flow results in poor heat transfer and inefficient evaporation of the aerosol. The exiting mean geometric diameter is 1.83 μm. In contrast, outlet flow of 15 L/min results in excellent spreading of the aerosol through the heat exchanger region. The resulting mean geometric diameter is 0.35 μm at exit, which indicates full drying of the initial 3.9-μm droplets, and the predicted DF is approximately 10%. DFs and geometric exit diameters are reported in Table 1 for the improved mixer with inlet temperatures of 45°C and 50°C. DFs are based on drug mass and include the mixer unit along with 50 cm of outlet tubing. It appears that the improved mixer is capable of delivering fully dried submicrometer particles at flow rates of 10 and 15 L/min, consistent with nasal HFT and NPPV, with DFs of approximately 10% or less (Table 1).

As reported in Table 1, RH conditions are below 100% for the aerosol delivery line in order to quickly form the submicrometer aerosol. A set water mass is available from the evaporating droplets, and the temperature of the aerosol stream determines the humidity value. It is expected that the inhalation of, for example, 33°C air and 60% RH will not excessively dry the airways due to the amount of water mass in the air. Furthermore, aerosol administration periods with ECG delivery are expected to be brief, *e.g.*, 1–5 min. If increasing the RH is required, Table 1 illustrates that reducing the inlet mixer temperature increases RH values while still producing a submicrometer aerosol. Furthermore, simply using a nebulizer with a higher liquid output rate, such as the Aeroneb Pro (Aerogen), can significantly raise the inhaled RH value if needed.

Nasal cannula

Trajectories of aerosols delivered through the Optiflow nasal cannula along with deposition locations for 6,000 particles are illustrated in Figure 6. For 900-nm particles, a relatively even distribution of the trajectories is observed to exit the two nasal prongs. The CFD predicted DF of 20.5% in the cannula and 20 cm of inlet tubing is in close agreement with the drug deposition observed *in vitro* of 16.4% (SD = 5.8%). The conventional 4.7-μm aerosol produced very high depositional losses with a CFD value of 74.2% and an *in vitro* value of 67.6% (SD = 3.9%). Clearly, use of the submicrometer aerosol is a significant improvement compared with conventional sizes. However, depositional losses for all particle sizes considered are above the 10% criterion even for this relatively large-bore cannula.

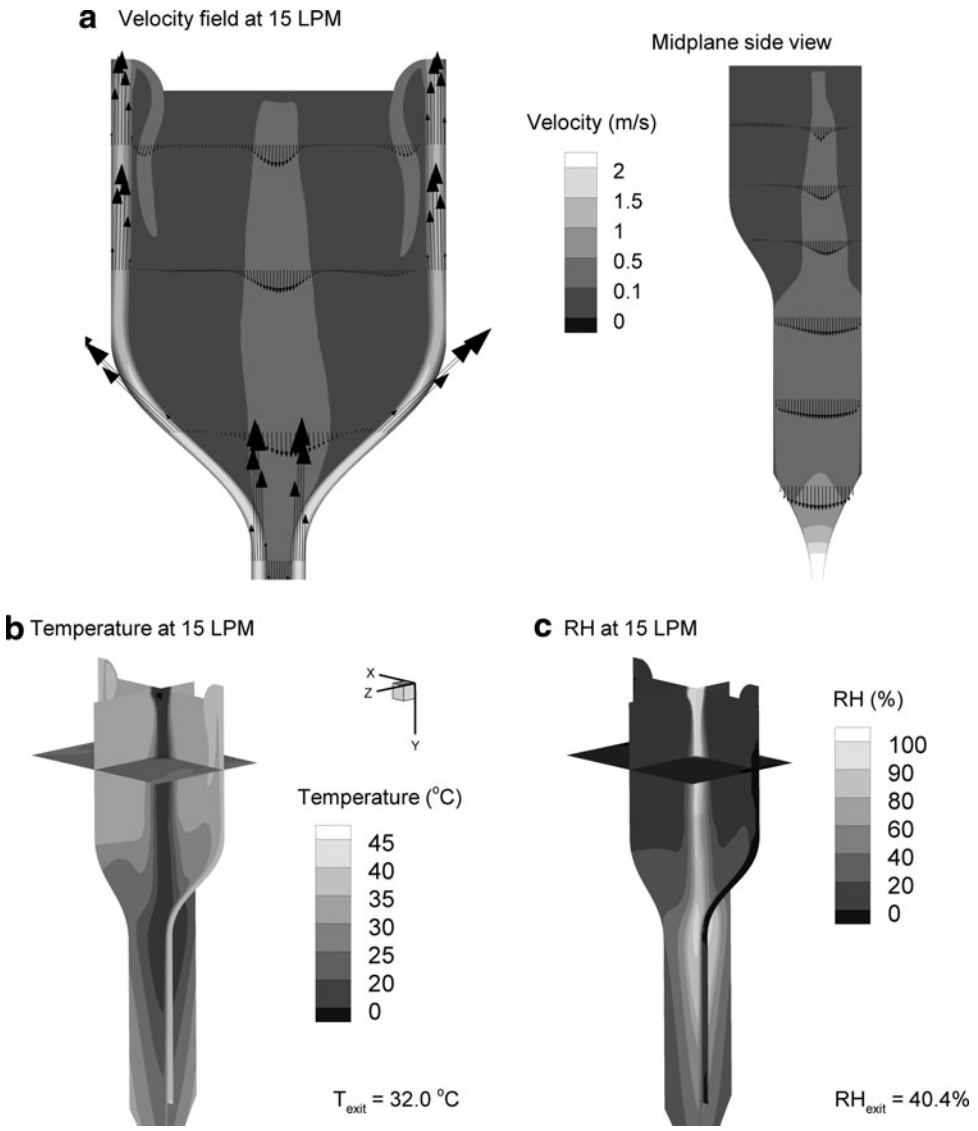

FIG. 4. Continuous-phase characteristics in the improved mixer at selected cross-sectional planes in terms of **(a)** contours of velocity magnitude and velocity vectors, **(b)** the temperature field, and **(c)** RH conditions for an aerosol outlet flow rate of 15 L/min.

Table 1. Predicted Outlet Conditions and DFs for the Improved Aerosol Mixer

Airflow conditions	*Temperature (°C)*	*RH (%)*	d_{geo} *(μm)*	*DF (%)*
45°C inlet air				
5 L/min	24.1	100.0	1.83	4.7
10 L/min	30.0	65.4	0.35	8.9
15 L/min	32.0	40.4	0.35	9.9
50°C inlet air				
5 L/min	29.3	96.1	1.73	5.7
10 L/min	33.2	60.0	0.35	9.2
15 L/min	36.6	33.2	0.35	10.3

The data presented are the predicted outlet conditions and DFs for the improved aerosol mixer at two different inlet airstream temperatures (45°C and 50°C) and outlet flow rates of 5, 10 and 15 L/min. The mean geometric diameter of the aerosol at the exit of the mixer and 50 cm of tubing is reported as d_{geo}.

Trajectories and deposition locations for the D and DS cannulas are illustrated in Figures 7 and 8, respectively, at a flow rate of 15 L/min through the aerosol inlet. Abrupt changes in flow direction in the D cannula result in recirculation and particle impaction on most surfaces, especially for the larger 3.9-μm aerosol (Fig. 7). In contrast, the DS design significantly reduces deposition for both the submicrometer and micrometer aerosol particles (Fig. 8). Deposition fractions with the DS geometry and a delivery flow rate of 15 L/min are 7.3% and 20.9% for the 900-nm and 3.9-μm particles, respectively. Therefore, the DS design reduces deposition in the cannula by a factor of 3–4 compared with the D model for both particle sizes at a flow rate of 15 L/min.

DFs for the three cannulas at flow rates of 2–15 L/min over a range of submicrometer and micrometer particle sizes are presented in Figure 9, based on CFD predictions. In general, DFs are lower in the Optiflow geometry than in the D cannula, because two prongs are available in the former to deliver the aerosol at each flow rate. Both the D and DS models deliver the aerosol through one prong for use with ECG delivery. For most cases with submicrometer aerosols,

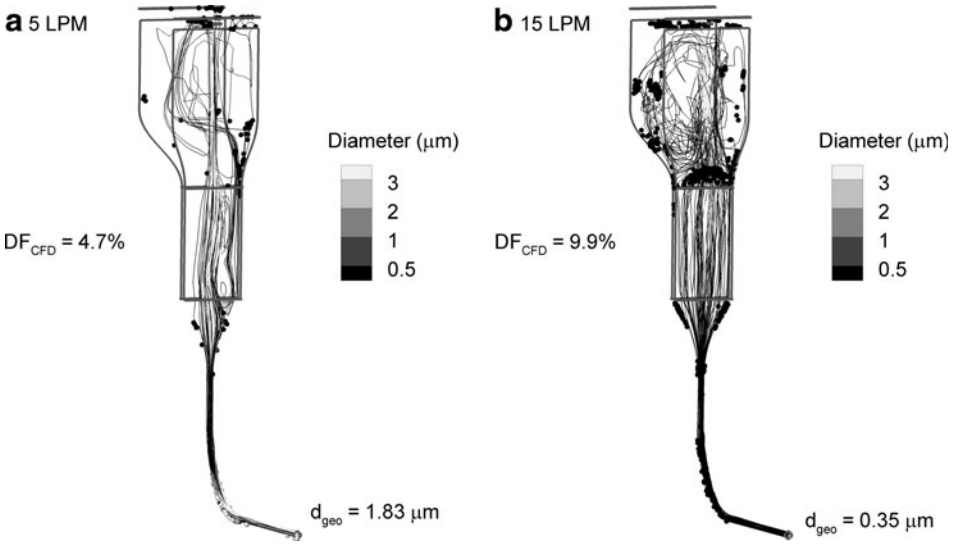

FIG. 5. Trajectories colored according to changing droplet size in the improved mixer, particle deposition locations (spheres on the geometry surface), and DFs (%) for aerosol transport flow rates of **(a)** 5 and **(b)** 15 L/min. For both flow rates, DFs are less than 10%; however, evaporation to submicrometer size is only observed at the higher flow rate.

the DS design reduces DFs compared with the Optiflow cannula by a factor of approximately 2 and compared with the D cannula by a factor of approximately 3. With the larger micrometer aerosols and the DS cannula, operation at 2 L/min appears to meet the 10% (or under) DF target (Fig. 9a). The DS model is capable of delivering all aerosols at DFs below 10% at 5 L/min and below 20% at 10 and 15 L/min (Fig. 9b–d). As a result, the DS cannula greatly improves the delivery efficiency of micrometer aerosols to the nose at low and high flow rates. However, achieving effective delivery rates of 90% and greater at flow rates consistent with adult HFT requires the use of submicrometer particles and the DS design.

Experimental verification of CFD results

For experimental verification of CFD results, the improved mixer and DS cannula were constructed using a rapid prototyping approach. It was determined that placing the internal Kapton heaters on the metal plates (gas delivery side) provided the required energy to heat the airstream and fully evaporate the aerosol. Use of internal heaters also eliminated the need for excess heated air, such that a sealed system design could be implemented. As a result, this sealed system with internal heaters was constructed and tested in the experiments. The design is identical to the CFD simulations in all regions of aerosol transport including the mixer, heat-transfer region, outlet tubing, and DS cannula.

Based on the dried aerosol size correlations provided by Longest et al.,[23] an AS concentration of 1.06% w/v was predicted to produce a target size of 900-nm dried particles exiting the improved mixer tubing. Preliminary experiments indicated that with this concentration, the exit mean MMAD of the dried particles was approximately 1 μm, which was slightly higher than the target 900-nm aerodynamic size. Optimization of the drug concentration was then performed to find the AS concentration to produce an aerosol with the mean MMAD of 900 nm. Results indicated that an AS concentration of 0.2% w/v reliably produced a dried aerosol with an MMAD of 900 nm (SD = 0.0). The mean (SD) geometric standard deviation of the aerosol was 1.9 (0.0) ($n = 5$). This lower mass fraction compared with the predicted value is likely due to polydisperse effects of the aerosol, whereas the correlations were based on a monodisperse approximation, as well as changes to the nebulizer output as the solute concentration is reduced.

For a mixer flow rate of approximately 15 L/min and a nebulizer solution concentration of 0.2% w/v AS (producing a 900-nm MMAD dried aerosol), Table 2 reports experimentally determined drug DFs in sections of the mixer system, connective tubing, and DS nasal cannula. CFD results of DF are also provided in this table for a solution concentration

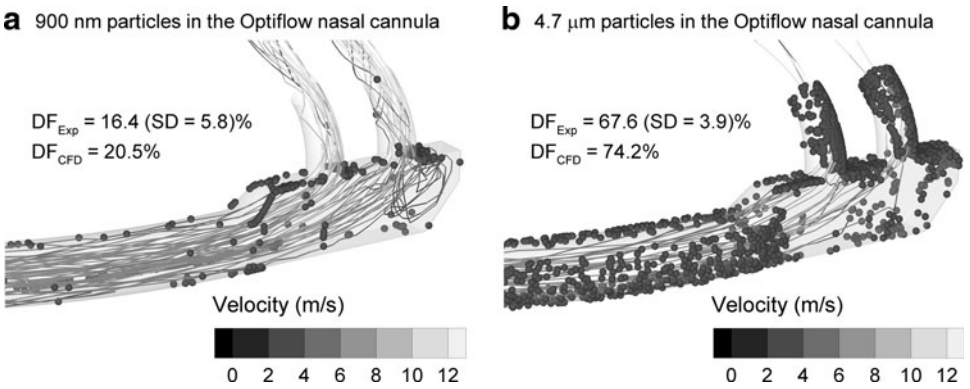

FIG. 6. Comparison of experimental and CFD predictions of DF in the Optiflow nasal cannula and 20 cm of 10-mm diameter inlet tubing for a flow rate of 20 L/min and particle sizes of **(a)** 900 nm and **(b)** 4.7 μm. Particle trajectories are contoured according to velocity, and particle deposition locations are illustrated based on CFD predictions.

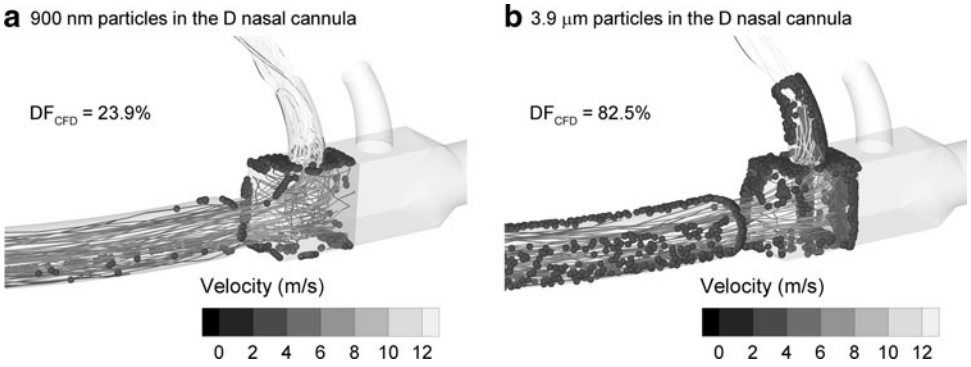

FIG. 7. Particle trajectories shaded according to velocity, deposition locations, and CFD predicted DFs at 15 L/min through the aerosol inlet for **(a)** 900- and **(b)** 3.9-μm particles in the D cannula and 20 cm of 10-mm diameter inlet tubing.

of 0.1% (consistent with the simulations reported above) and 900-nm dried particles in the cannula. As with the radial mixer design, DFs in the improved mixer are based on the difference between the nominal dose and the total recovered dose. Therefore, it is assumed that any drug not recovered during the washing of the other device deposition sites is deposited in the mixer. The *in vitro* results confirm that the drug DF in the improved mixer plus 50 cm of tubing ($DF_{total} = 10.5\%$) and cannula plus 20 cm of tubing ($DF_{total} = 1.2\%$) is very low and meets the goal of approximately 10% or less deposition in each region. For the improved mixer and exit tubing, the *in vitro* DF (10.5%) is in very close agreement with the CFD predictions (DF = 9.9%). Considering the cannula and 20 cm of inlet tubing, the experimental deposition results (DF = 1.2%) are much lower than the CFD predictions (DF = 7.3%). As a result, the CFD model represents an upper bound of potential deposition in the DS case. It is noted that CFD predictions in the Optiflow cannula for the 900-nm aerosol were very similar to the *in vitro* predictions [$DF_{Exp} = 16.5\%$ (5.8%) vs. $DF_{CFD} = 20.5\%$].

Discussion

A primary outcome of this study is that a submicrometer aerosol can be formed using a conventional mesh nebulizer and delivered through a nasal cannula in a highly efficient manner. CFD predicted depositional losses in the improved mixer (with 50 cm of connective tubing) and nasal cannula (with 20 cm of tubing) to total approximately 17%, which is below the target of 10% in each of the two devices. The improved mixer produced a submicrometer particle at flow rates consistent with adult nasal HFT and NPPV. In the verification experiments, total system deposition (mixer, all tubing, and cannula) was 11.7% and a submicrometer aerosol with an MMAD = 900 nm was formed, which was the initial target size for the aerosol. At flow rates consistent with high-flow nasal ventilation, the improved mixer reduced aerosol depositional losses by a factor of approximately 3 compared with an initial design. The DS nasal cannula reduced the deposition of submicrometer aerosols by a factor of 2–3 compared with the D and Optiflow models based on CFD results. Considering the experiments, the DS design reduced submicrometer particle cannula loss by a factor greater than 10 compared with the commercial Optiflow. The developed system appears to be effective for providing high-efficiency delivery of submicrometer aerosols to adults receiving HFT or NPPV with nasal cannula interfaces.

Selection of the mixer may depend on the intended method for respiratory drug delivery. It was observed that the improved mixer did not produce a submicrometer aerosol at 5 L/min, but a final exit size of approximately 1.8 μm was achieved. This was because the core of aerosol flow did not spread in the heat exchanger region, making heat transfer inefficient. In contrast, Longest *et al.*[23] reported that at 5 L/min the radial mixer with 1 m of counterflow heated tubing produced a submicrometer aerosol ($d_{geo} = 0.69$ μm). As a result, the radial mixer may be advantageous for producing submicrometer aerosols during low-flow delivery (~1–5 L/min)

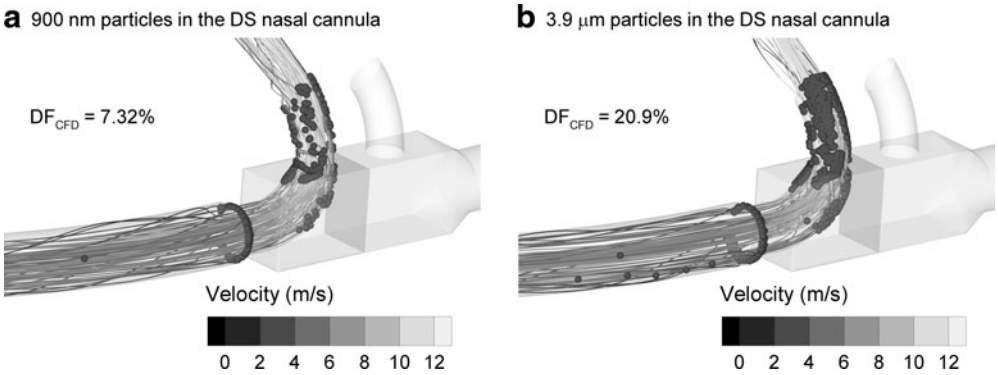

FIG. 8. Particle trajectories shaded according to velocity, deposition locations, and CFD predicted DFs at 15 L/min through the aerosol inlet for **(a)** 900- and **(b)** 3.9-μm particles in the DS cannula and 20 cm of 10-mm diameter inlet tubing.

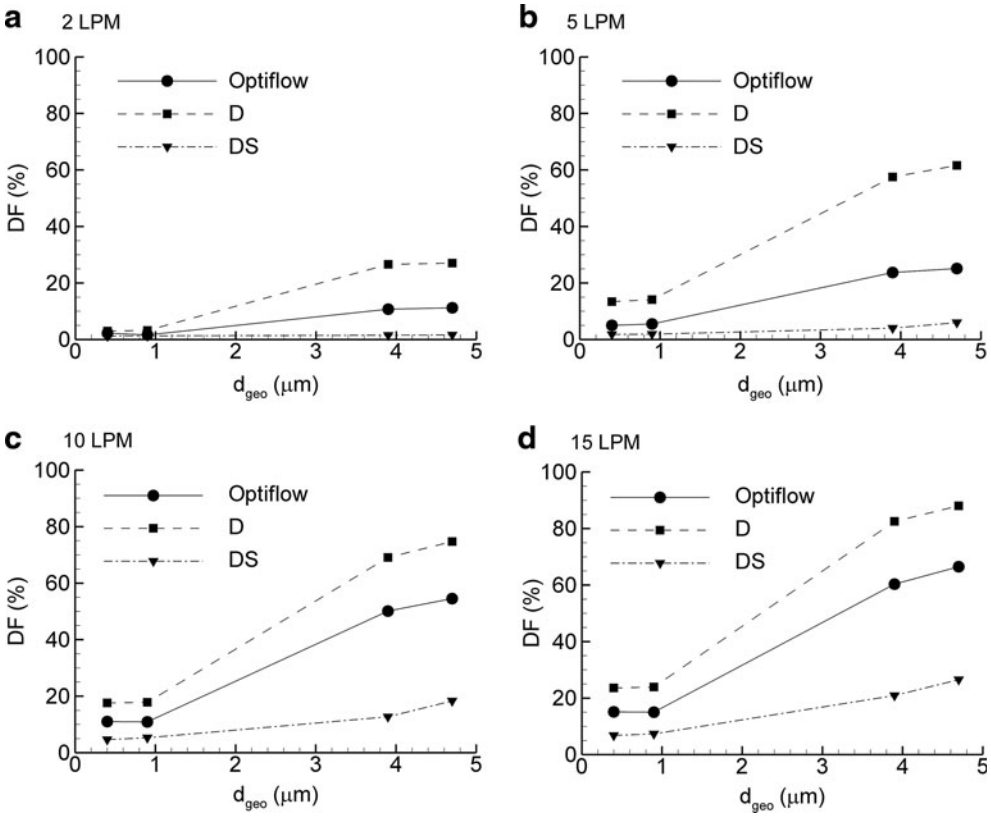

FIG. 9. DFs (%) in the nasal cannula geometries and 20 cm of connective inlet tubing as a function of particle size for aerosol flow rates of **(a)** 2, **(b)** 5, **(c)** 10, and **(d)** 15 L/min.

or with pediatric patients. However, additional advantages of the improved mixer include a vertical orientation, compact heat exchanger region, and one input air line. Including Kapton film heaters inside the heat-exchange region also improved the design. At a flow rate of 5 L/min for a 1.8-μm aerosol, the total DFs in both the improved mixer (~5%) and DS cannula (~2%) were very low. Furthermore, nasal deposition of a 1.8-μm particle at 5 L/min will also be low. Nasal deposition, however, will increase if the patient inhales nasally at a rate greater than the HFT gas flow. Based on these observations, it may be advantageous to use the improved mixer for ECG delivery at low flows even if the aerosol is not fully dried. A submicrometer aerosol size can be achieved with the optimal mixer and low flow rates by decreasing the width of the heat exchanger channel (<1.2 cm) to provide better spreading of the aerosol and improve heat transfer. However, this distance was not decreased in the current study, as it will increase deposition at higher flow rates.

Table 2. DFs of Drug Mass in the Aerosol Generation and Delivery System Based on Both *In Vitro* Experiments and CFD Predictions

	DF of drug mass (%)	
Region	In vitro *experiments*	*CFD predictions*
Nebulizer inlet	0.7 (0.3)[a]	
Improved mixer	8.2[b] (2.1)	
50 cm of tubing out of the mixer	1.6 (0.3)	
Nebulizer inlet + mixer + tubing	10.5	9.9
20 cm of tubing at cannula inlet	0.6 (0.2)	
DS cannula	0.6 (0.2)	
Tubing + DS cannula	1.2	7.3

[a]SD values are shown in parentheses for $n \geq 4$ experiments.
[b]Deposition in the mixer was estimated as the difference between the nominal delivered dose and the total recovered dose. Deposition in all other components was based on washing and HPLC analysis.

The focus of this study was on the formation of submicrometer aerosols for ECG nasal delivery with high flow rates in adults. However, low flow rates were also considered in the nasal cannula models. These data can be implemented to explore appropriate cannula designs and particle-size selection for nasal delivery during low-flow applications, for the use of conventional aerosol sizes, or for applications with pediatric patients. It is interesting that the adult Optiflow cannula can deliver conventional-sized aerosol with a DF of approximately 10% at 2 L/min and approximately 20% at 5 L/min. These depositional loss values are reduced by a factor of approximately 4 with the DS cannula. At higher flow rates of 10 and 15 L/min, the DS cannula can deliver conventional aerosols with DFs of approximately 20% and below. However, it should be realized that these depositional losses are just in the nasal cannula with 20 cm of tubing. Deposition in longer delivery lines of these conventional-sized aerosols will be large due to sedimentation at low flow rates and impaction at high flow rates. Deposition in the nasal cavity is also high for conventional-sized aerosols during inhalation or high flow. For example, experiments reported in Longest *et al.*[15] indicated that a 4.7-μm particle inhaled with a nasal flow rate of 30 L/min

resulted in approximately 70% NMT deposition, even with some evaporation of the aerosol. As a result, delivery of conventional-sized aerosols through nasal cannula appears possible, which is consistent with the findings of Bhashyam *et al*.[11] and Ari *et al*.[12] Use of the DS design presented in this study will significantly improve one source of depositional loss for micrometer aerosols. However, the delivery of conventional-sized aerosols through a nasal cannula creates high deposition in the generation device, delivery lines, and nasal cavity. In contrast, delivery with ECG and submicrometer aerosols provides low deposition in the device, connectors, tubing, cannula, and nasal passage relatively independent of flow rate. Therefore, it appears that the ECG approach consistently provides for higher delivery efficiency with less variability compared with conventional-sized aerosols.

One concern with the formation and use of submicrometer aerosols is the rate of drug delivery and time required to receive an effective dose. In the experiments, the solution concentration of AS was reduced to 0.2% w/v to form an aerosol with an MMAD of 900 nm. Typical nebulized solutions of AS or corticosteroids contain 0.02–0.5% w/v of drug. Therefore, the solution concentration of 0.2% w/v is within the range of typical clinical values. In our studies with the Aeroneb Lab nebulizer, the liquid delivery rate is 0.2 mL/min.[23] For a solution concentration of 0.2% w/v, the resulting drug nebulization rate is 400 μg/min. It is interesting to compare the time required to deliver a typical 500-μg dose using a solution concentration of 0.2% w/v to the lungs via the nose with a conventional system versus the optimized mixer and nasal cannula developed in this study. With a conventional system and HFT conditions, depositional losses will result in only 1–10% of the nebulized dose reaching the lungs. Using the optimized mixer, nasal cannula, and ECG delivery, 90% of the dose can be delivered to the lungs based on findings of this study. As a result, the conventional system with the Aeroneb Lab nebulizer will require between 12.5 and 125 min to deliver the 500-μg dose to the lungs. In contrast, the optimized system developed in this study will require approximately 1.4 min. Therefore, the optimized system is capable of delivering a set dose to the lungs via the nose 1–2 orders of magnitude faster than a conventional delivery approach.

An increasing body of evidence indicates that, with ECG delivery, sufficient droplet growth is achieved within the airways to foster full aerosol deposition. For oral ECG using a dual-flow mouthpiece, Tian *et al*.[19] demonstrated that increase of an initially submicrometer aerosol to sizes greater than 3 μm was possible during an inhalation cycle and that the resulting micrometer aerosol was fully retained within the lungs. Hindle *et al*.[18] reported concurrent *in vitro* and CFD results that showed submicrometer aerosol size increases to conventional values (2 μm and above) and that tracheobronchial deposition increases by an order of magnitude with oral ECG delivery. For nasal ECG delivery with separate aerosol and humidity streams, Longest *et al*.[15] demonstrated submicrometer size increase to approximately 2 μm within the trachea with the potential for continued aerosol growth as the flow enters the lungs. Aerosol size increase can be further enhanced by including hygroscopic excipients in the formulation, which is referred to as excipient enhanced growth (EEG).[20–22,34] Recent studies have demonstrated that the RH within the airways is sufficient to foster submicrometer size increase with EEG to micrometer sizes (2–3 μm and greater), which results in full lung deposition of the aerosol for oral inhalation.[21,35] Future studies are needed to explore the growth kinetics and sites of regional deposition within the airways for nasally administered aerosols using either the ECG or EEG approaches. However, the current study provides a method for effectively generating the required submicrometer aerosols and delivering the medication to the patient with a very high efficiency ($\sim$90%) using a nasal cannula interface.

Limitations of the current analysis compared with *in vivo* applications include steady flow through the system, a single configuration of the delivery lines, and a single nasal cannula size. Based on the excess exhaust and recirculation design of the system, exhalation will increase downstream resistance and decrease the amount of flow through the system. However, operation in the range of 10–15 L/min outflow produced fully dried submicrometer particles (Table 1). Furthermore, RH values below 60% indicate that additional evaporation is possible for changes in number concentration associated with cyclic changes in aerosol throughput. Maintaining high-efficiency delivery through the nasal passages during exhalation may require only generating the aerosol during inhalation, as with the study of Nikander *et al*.[36] Deposition in the delivery lines of micrometer particles will depend on the configuration and curvature of the tubes. However, submicrometer particles will have very low depositional losses in the delivery tubes for practical radii of curvature. Finally, only large-bore adult cannulas were considered with dimensions similar to the medium-sized adult Optiflow nasal cannula. Bhashyam *et al*.[11] previously showed that depositional losses in cannulas were different for infant, pediatric, and adult sizes. However, these differences are expected to be minimized with the use of submicrometer aerosols.

In conclusion, this study has developed an effective generation and delivery system for producing submicrometer aerosols from conventional mesh nebulizers that demonstrates low deposition in the aerosol mixer and nasal cannula devices. Total depositional losses were below 10% in both the improved aerosol mixer and DS nasal cannula even at high delivery rates, based on *in vitro* experiments and CFD simulations. The resulting delivery efficiency of the aerosol from the nebulizer through the improved nasal cannula is greater than 80% based on CFD simulations and near 90% based on *in vitro* experiments. This represents a significant improvement to previous reports of maximum cannula delivery, which were in the range of 11%[12] to 27%[11] at very low flow rates (2–3 L/min). The DS nasal cannula significantly improved the delivery of both submicrometer and micrometer aerosols. The use of CFD simulations combined with *in vitro* experiments accelerated the design and development process for the system and verified functionality. Future studies are needed to explore the effects of cyclic inhalation and exhalation as well as deposition in the nasal airways.

Acknowledgments

This study was supported by Award R01 HL107333 from the National Heart, Lung, and Blood Institute. The content is

solely the responsibility of the authors and does not necessarily represent the official views of the National Heart, Lung, and Blood Institute or the National Institutes of Health.

Author Disclosure Statement

No conflicts of interest exist.

References

1. Lightowler JV, Wedzicha JA, Elliott MW, and Ram FSF: Non-invasive positive pressure ventilation to treat respiratory failure resulting from exacerbations of chronic obstructive pulmonary disease: Cochrane systematic review and meta-analysis. BMJ. 2003;326:185–187.
2. Rea H, McAuley S, Jayaram L, Garrett J, Hockey H, Storey L, O'Donnell G, Haru L, Payton M, and O'Donnell K: The clinical utility of long-term humidification therapy in chronic airway disease. Respir Med. 2010;104:525–533.
3. Aboussouan LS, and Ricaurte B: Noninvasive positive pressure ventilation: increasing use in acute care. Cleve Clin J Med. 2010;77:307–316.
4. Parke RL, McGuinness SP, and Eccleston ML: A preliminary randomized controlled trial to assess effectiveness of nasal high-flow oxygen in intensive care patients. Respir Care. 2011;56:265–270.
5. Dysart K, Miller TL, Wolfson MR, and Shaffer TH: Research in high flow therapy: mechanisms of action. Respir Med. 2009;103:1400–1405.
6. Price AM, Plowright C, Makowski A, and Misztal B: Using a high-flow respiratory system (Vapotherm) within a high dependency setting. Nurs Crit Care. 2008;13:298–304.
7. Roca O, Riera J, Torres F, and Masclans JR: High-flow oxygen therapy in acute respiratory failure. Respir Care. 2010; 55:408–413.
8. Hess DR: The mask of noninvasive ventilation: principles of design and effects on aerosol delivery. J Aerosol Med. 2007; 20:S85–S99.
9. Dhand R: Aerosol delivery during mechanical ventilation: from basic techniques to new devices. J Aerosol Med Pulm Drug Deliv. 2008;21:45–60.
10. Dhand R: Aerosol therapy in patients receiving noninvasive positive pressure ventilation. J Aerosol Med Pulm Drug Deliv. 2012;25:63–78.
11. Bhashyam AR, Wolf MT, Marcinkowski AL, Saville A, Thomas K, Carcillo JA, and Corcoran TE: Aerosol delivery through nasal cannulas: an *in vitro* study. J Aerosol Med Pulm Drug Deliv. 2008;21:181–187.
12. Ari A, Harwood R, Sheard M, Dailey P, and Fink JB: In vitro comparison of heliox and oxygen in aerosol delivery using pediatric high flow nasal cannula. Pediatr Pulmonol. 2011; 46:795–801.
13. Cheng YS: Aerosol deposition in the extrathoracic region. Aerosol Sci Technol. 2003;37:659–671.
14. Garcia GJM, Tewksbury EW, Wong BA, and Kimbell JS: Interindividual variability in nasal filtration as a function of nasal cavity geometry. J Aerosol Med Pulm Drug Deliv. 2009;22:139–155.
15. Longest PW, Tian G, and Hindle M: Improving the lung delivery of nasally administered aerosols during noninvasive ventilation: an application of enhanced condensational growth (ECG). J Aerosol Med Pulm Drug Deliv. 2011;24: 103–118.
16. Dhand R: Inhalation therapy in invasive and noninvasive mechanical ventilation. Curr Opin Crit Care. 2007;13: 27–38.
17. Longest PW, McLeskey JT, and Hindle M: Characterization of nanoaerosol size change during enhanced condensational growth. Aerosol Sci Technol. 2010;44:473–483.
18. Hindle M, and Longest PW: Evaluation of enhanced condensational growth (ECG) for controlled respiratory drug delivery in a mouth–throat and upper tracheobronchial model. Pharm Res. 2010;27:1800–1811.
19. Tian G, Longest PW, Su G, and Hindle M: Characterization of respiratory drug delivery with enhanced condensational growth (ECG) using an individual path model of the entire tracheobronchial airways. Ann Biomed Eng. 2011;39: 1136–1153.
20. Hindle M, and Longest PW: Condensational growth of combination drug-excipient submicrometer particles for targeted high efficiency pulmonary delivery: evaluation of formulation and delivery device. J Pharm Pharmacol. 2012; 64:1254–1263.
21. Longest PW, and Hindle M: Numerical model to characterize the size increase of combination drug and hygroscopic excipient nanoparticle aerosols. Aerosol Sci Technol. 2011;45:884–899.
22. Longest PW, and Hindle M: Condensational growth of combination drug-excipient submicrometer particles: comparison of CFD predictions with experimental results. Pharm Res. 2012;29:707–721.
23. Longest PW, Spence BM, Holbrook LT, Mossi KM, Son Y-J, and Hindle M: Production of inhalable submicrometer aerosols from conventional mesh nebulizers for improved respiratory drug delivery. J Aerosol Sci. 2012;51:66–80.
24. Longest PW, and Hindle M: CFD simulations of enhanced condensational growth (ECG) applied to respiratory drug delivery with comparisons to in vitro data. J Aerosol Sci. 2010;41:805–820.
25. Longest PW, and Hindle M: Evaluation of the Respimat Soft Mist inhaler using a concurrent CFD and *in vitro* approach. J Aerosol Med Pulm Drug Deliv. 2009;22:99–112.
26. Longest PW, Hindle M, Das Choudhuri S, and Byron PR: Numerical simulations of capillary aerosol generation: CFD model development and comparisons with experimental data. Aerosol Sci Technol. 2007;41:952–973.
27. Longest PW, and Vinchurkar S: Validating CFD predictions of respiratory aerosol deposition: effects of upstream transition and turbulence. J Biomech. 2007;40:305–316.
28. Wilcox DC: *Turbulence Modeling for CFD*, 2nd ed. DCW Industries, Inc., La Cañada, CA; 1998.
29. Longest PW, and Xi J: Condensational growth may contribute to the enhanced deposition of cigarette smoke articles in the upper respiratory tract. Aerosol Sci Technol. 2008;42:579–602.
30. Longest PW, and Xi J: Effectiveness of direct Lagrangian tracking models for simulating nanoparticle deposition in the upper airways. Aerosol Sci Technol. 2007;41: 380–397.
31. Matida EA, Finlay WH, and Grgic LB: Improved numerical simulation of aerosol deposition in an idealized mouth–throat. J Aerosol Sci. 2004;35:1–19.
32. Longest PW, Hindle M, Das Choudhuri S, and Xi J: Comparison of ambient and spray aerosol deposition in a tandard induction port and more realistic mouth–throat geometry. J Aerosol Sci. 2008;39:572–591.

33. Vinchurkar S, and Longest PW: Evaluation of hexahedral, prismatic and hybrid mesh styles for simulating respiratory aerosol dynamics. Comput Fluids. 2008;37:317–331.
34. Longest PW, Tian G, Li X, Son Y-J, and Hindle M: Performance of combination drug and hygroscopic excipient submicrometer particles from a Softmist inhaler in a characteristic model of the airways. Ann Biomed Eng. 2012. [Epub ahead of print]
35. Tian G, Longest PW, Li X, and Hindle M: Targeting aerosol deposition to and within the lung airways using excipient enhanced growth. J Aerosol Med Pulm Drug Deliv. 2012 (in press).
36. Nikander K, Prince I, Coughlin S, Warren S, and Taylor G: Mode of breathing-tidal or slow and deep-through the I-neb adaptive delivery (ADD) system affects lung deposition of ^{99m}Tc-DTPA. J Aerosol Med Pulm Drug Deliv. 2010;23(S1):S37–S43.

Received on August 21, 2012
in final form, October 31, 2012

Reviewed by:
Timothy Corcoran
Li Zheng

Address correspondence to:
Dr. P. Worth Longest
Virginia Commonwealth University
401 West Main Street
P.O. Box 843015
Richmond, VA 23284-3015

E-mail: pwlongest@vcu.edu